



BNL-93722-2010-IR

***Carbonation of Rock Minerals by Supercritical
Carbon Dioxide at 250°C***

Toshifumi Sugama, Lynne Ecker, Thomas Butcher

June 2010

Energy Resources Department/Energy Resources Division

Brookhaven National Laboratory

P.O. Box 5000
Upton, NY 11973-5000
www.bnl.gov

Notice: This manuscript has been authored by employees of Brookhaven Science Associates, LLC under Contract No. DE-AC02-98CH10886 with the U.S. Department of Energy. The publisher by accepting the manuscript for publication acknowledges that the United States Government retains a non-exclusive, paid-up, irrevocable, world-wide license to publish or reproduce the published form of this manuscript, or allow others to do so, for United States Government purposes.

DISCLAIMER

This report was prepared as an account of work sponsored by an agency of the United States Government. Neither the United States Government nor any agency thereof, nor any of their employees, nor any of their contractors, subcontractors, or their employees, makes any warranty, express or implied, or assumes any legal liability or responsibility for the accuracy, completeness, or any third party's use or the results of such use of any information, apparatus, product, or process disclosed, or represents that its use would not infringe privately owned rights. Reference herein to any specific commercial product, process, or service by trade name, trademark, manufacturer, or otherwise, does not necessarily constitute or imply its endorsement, recommendation, or favoring by the United States Government or any agency thereof or its contractors or subcontractors. The views and opinions of authors expressed herein do not necessarily state or reflect those of the United States Government or any agency thereof.

Carbonation of Rock Minerals by Supercritical Carbon Dioxide at 250°C

Prepared for

**The U.S. Department of Energy
Energy Efficiency and Renewable Energy
Geothermal Technologies Program
1000 Independence Avenue SW
Washington, D.C. 20585**

Prepared by

T. Sugama, L. Ecker, and T. Butcher

**Energy Science & Technology Department
Brookhaven National Laboratory
Upton, NY 11973-5000**

June 2010

Notice: This manuscript has been authored by employee of Brookhaven Science Associates, LLC under Contract No. DE-AC02-98CH 10886 with the U.S. Department of Energy. The publisher by accepting the manuscript for publication acknowledges that the United States Government retains a non-exclusive, paid-up, irrevocable, world-wide license to publish or reproduce the published form of this manuscript, or allow others to do so, for the United States Government purposes.

Abstract

Wet powder-samples of five rock minerals, granite, albite, hornblende, diorite, and biotite mica, were exposed in supercritical carbon dioxide (scCO₂) for 3 days at 250°C under 17.23 MPa pressure, and then the susceptibility of the various crystalline phases present in these mineral structures to reactions with hot scCO₂ was investigated by XRD and FT-IR. The anorthite present in diorite was identified as the most vulnerable phase to carbonation. In contrast, biotite displayed a great resistance, although its phase was transformed hydrothermally to sanidine and quartz. Granite comprised of two phases, anorthoclase-type albite and quartz. The carbonation of former phase led to the formation of amorphous sodium and potassium carbonates coexisting with the clay-like by-products of the carbonation reaction. The reactivity of quartz to scCO₂ was minimal, if any. Among these rock minerals, only hornblende formed crystalline carbonation products, such as calcite and magnesite after exposure, reflecting the likelihood of an increase in its volume. Based upon the feldspar ternary diagram, the carbonation rate of various different minerals in the plagioclase feldspar family depended primarily on the amount of anorthite. On the other hand, alkali feldspar minerals involving anorthoclase-type albite and sanidine had a lower reactivity with scCO₂, compared with that of plagioclase feldspar minerals.

Introduction

Unlike conventional geothermal technology, enhanced geothermal system (EGS) is new type of technology that allows us to extract hydrothermal energy at any location having underground temperatures of $\geq 200^{\circ}\text{C}$ across the United States and worldwide [1]. The distinctive technological feature of EGS, compared with that of conventional technology, lies in creating a hydrothermal reservoir in an impermeable hot rock layer rather than tapping of natural reservoir aquifers at the temperatures up to 350°C , which may be located as deep as 10 km. As far as the reservoir rock temperature is more than 200°C , EGS offers the possibility of constructing the geothermal well at a relatively shallow location, ~ 5 km below surface or less [2-4].

To create a reservoir, water or chemicals from an injection well must be pumped into a hot rock layer at high pressure and a high flow rate. Such hydraulic- and chemical-stimulations are essential both in initiating the development of new fractures and opening the rock's pre-existing fractures [5,6]. The continued pumping of water and chemicals as fracturing fluids creates multiple-fractures and leads to their propagation; it assures the formation of ideal reservoir consisting of a three dimensional-network structure of fractures. After creating the reservoir, production well is installed in the fracture network structure. Then, the heat transmission fluid as working fluid from the injection well is transported to the production well through the hot fracture zones under a high pressure, and further it circulates between the injection- and production-wells.

Supercritical carbon dioxide (scCO_2) has attractive potential as an alternative working fluid because of its excellent heat uptake and transmission, and its high flow rate relative to its low density, compared with that of water [7]. At present, scCO_2 have been applied extensively to old oil wells to enhance recovery of residual- and additional- oil under pressures above 1,070 psi (7.38MPa) at the critical point of CO_2 [8,9]. Its use in enhanced oil recovery (EOR) is becoming increasingly popular in worldwide. In addition, the EOR process technology is very similar to that of EGS; namely, the scCO_2 is supplied from an injection well and then it is taken up by a production well.

Despite the promise of scCO₂, one serious concern is its proclivity to carbonation of the reservoir's rock minerals at temperatures $\geq 200^{\circ}\text{C}$. Our previous study of the mechanism of high-temperature carbonation of well-casing cementitious materials strongly demonstrated that ordinary Portland cement (OPC)-based well cement was a very susceptible to reactions with CO₂ in an aqueous environment [10-12]. The calcium silicate hydrate phase responsible for strengthening and densifying the cement structure reacted exclusively with wet CO₂ to form two reaction products, calcium carbonate and silica gel, leading to the disintegration of cement emplaced in the well.

Based upon this information, our focus in this research was on studying the carbonation of representative rock minerals in the EGS wells by scCO₂/water combination. Among the pure rock minerals used in this study were granite, albite, biotite, hornblende, and diorite. The study included the phase identification of carbonation reaction products and their underlying reaction mechanisms.

Experimental

Five minerals, granite, albite, biotite, hornblende, and diorite, were obtained from Rockman's Trading Post, Inc. In preparing the samples for scCO₂-exposure test, all minerals were smashed and grounded for making the powders with a particle size of < 0.2 mm. The powders then were mixed with an appropriate amount of water to prepare mineral pasts. The water/powdered mineral ratios by weight were 19.1, 12.0, 9.7, 19.2, and 63.8 % for granite, albite, hornblende, diorite, and biotite, respectively. Then, the pasts were inserted into 1-cm diameter x 5-cm long quartz vials; the thickness of the past adhering to vial wall's surface was approximately 3 mm. The vials were exposed for 3 days in an autoclave containing scCO₂ at 250°C under the helium pressure of 2500 psi (17.23 MPa).

Thereafter, the samples were dried in an oven at 100°C for 24 hours to eliminate all moisture adsorbed in the samples. Two analytical tools, x-ray diffraction (XRD) and Fourier transform infrared spectroscopy (FT-IR), were employed to identify amorphous-

and crystalline-carbonation products, and to estimate the extent of the susceptibility of these minerals to reaction with scCO₂.

Results and Discussion

Granite

Figure 1 shows the different features of the x-ray diffraction patterns of granite before and after exposure to scCO₂. Unexposed granite contains two phases, anorthoclase-type albite [(Na,K)AlSi₃O₈] in the family of alkali feldspar, and quartz (SiO₂). When the granite was exposed, the feature of diffraction pattern differed from that of the unexposed one. The major difference was a decay of the intensity of all albite-related XRD lines, while the line intensity of quartz-associated d-spacing remained unchanged. This result strongly demonstrated that the albite phase was susceptible to the reactions with scCO₂/water at 250°C under a pressure of 17.23 MPa. In contrast, the susceptibility of quartz in granite to scCO₂/water reactions was negligible, compared with that of albite.

This information was supported by FT-IR studies using the same samples (Figure 2). A typical spectrum from unexposed granite showed the following absorption bands: At 2438 cm⁻¹ ascribed to O-H stretching vibration in H₂O, adsorbed to quartz; at 1978 and 1870 cm⁻¹, originating from the Si-O stretching mode in quartz [13], at 1611 cm⁻¹ due to adsorbed H₂O; at 1097 and 998 cm⁻¹, corresponding to the oxygen-bridging Si-O-Si asymmetric stretching and non oxygen-bridging Si-O⁻ stretching [14,15] in albite; and at the range from 776 to 725 cm⁻¹ assigned to Al-O stretching [16] in albite.

For exposed samples, the attention was paid to the appearance of two new absorption bands at 1568 and 1420 cm⁻¹, and the shift of non oxygen-bridging Si-O band to lower wavenumber site, from 998 to 923 cm⁻¹. Since the oxygen in this last band is linked directly to Na⁺ and K⁺ cations, its shift to the SiOH-related band site suggests that scCO₂ ruptured the linkage between SiO⁻ and Na⁺ or K⁺. Hence, there is no reason to doubt that the band at 1420 cm⁻¹ reflected the amorphous sodium and potassium carbonates, Na₂CO₃ and K₂CO₃ [17]. As is well documented [18,19], the reactions between CO₂ and

water lead to the formation of ionic carbonic acid, $\text{CO}_2 + \text{H}_2\text{O} \leftrightarrow \text{HCO}_3^- + \text{H}^+ \leftrightarrow \text{CO}_3^{2-} + 2\text{H}^+$. These carbonates might be formed through the following wet carbonation reaction of albite in the granite, $2(\text{Na,K})\text{AlSi}_3\text{O}_8 + 2\text{CO}_3^- + 4\text{H}^+ \rightarrow \text{Na}_2\text{CO}_3 + \text{K}_2\text{CO}_3 + \text{Al}_2\text{Si}_{6-x}\text{O}_{12-2x}(\text{OH})_4 + x\text{SiO}_2$. Some silicon dioxide may be precipitated as reaction by-products [20]. If so, the band at 1568 cm^{-1} might be associated with the formation of the clay-like mineral, $\text{Al}_2\text{Si}_{6-x}\text{O}_{12-2x}(\text{OH})_4$, containing SiOH groups as the amorphous carbonation by-product.

Albite

Figure 3 shows the XRD patterns of albite ($\text{NaAlSi}_3\text{O}_8$) in the category of plagioclase feldspar before and after exposure. As is seen, there was no significant change in line intensity of all albite-related d-spacings after exposure, seemingly demonstrating that its susceptibility to reactions with $\text{scCO}_2/\text{water}$ was lower than that of the anorthoclase-type albite in granite. In addition, no crystalline carbonation products formed.

However, the FT-IR spectrum of the exposed albite revealed the formation of the amorphous carbonate products as reflected in the presence of two carbonation-related absorption bands at 1546 and 1422 cm^{-1} , and also a shift of the non oxygen-bridging band from 960 to 915 cm^{-1} . Although the extent of its carbonation might well be lower than that of the anorthoclase-type albite in granite, it appears that the albite also underwent wet carbonation, forming both the amorphous sodium carbonate and clay-like by-products, $2\text{NaAlSi}_3\text{O}_8 + \text{CO}_3^- + 2\text{H}^+ \rightarrow \text{Na}_2\text{CO}_3 + \text{Al}_2\text{Si}_6\text{O}_{14}(\text{OH})_2$.

Hornblende

The XRD pattern for unexposed hornblende revealed that most of the d-spacing lines belonged to the hornblende [$\text{Ca}_2(\text{Mg,Fe,Al})_5(\text{Al,Si})_8\text{O}_{22}(\text{OH})_2$] (Figure 5). Upon exposure to scCO_2 , carbonation generated three crystalline reaction products. Among them, two were the carbonate products, such as calcite (CaCO_3) and magnesite (MgCO_3), and third may be due to iron (III) oxide, attributed to hematite (Fe_2O_3). This pattern did not show any Fe-related carbonation products like siderite (FeCO_3).

Meanwhile, the line intensity of all hornblende's d-spacings had markedly decayed, compared with those of the unexposed one, emphasizing that hornblende is very susceptible to reactions with scCO₂/water.

Correspondingly, the FT-IR spectrum (Figure 6) encompassed two pronounced absorption bands at 1536 and 1398 cm⁻¹ attributed to the carbonation by-products, and the Ca and Mg carbonates, respectively. Although the band at 864 cm⁻¹ is related to Si-O stretching in Si-OH groups, it should be noted that this band also overlaps the Ca and Mg carbonate-related band for exposed sample. Further, the new band at 747 cm⁻¹ is likely to be associated with these carbonates [21].

Diorite

As is evidenced from its XRD pattern (Figure 7), unexposed original diorite comprises three crystalline phases, anorthite (CaAl₂Si₂O₈), biotite [K(Fe,Mg)₃AlSi₃O₁₀(OH)₂], and quartz. The dramatic changes in pattern's future were observed from the exposed sample; in particular, all anorthite- and quartz-related d-spacings disappeared, while the biotite phase remained intact. Indeed, no other crystalline phases except for biotite were distinguishable in this pattern. Conceivably, the biotite present in diorite mineral can withstand in a harsh scCO₂ and hydrothermal environment at 250°C. More importantly, the magnitude of carbonation of anorthite in the plagioclase feldspar family was considerably higher than that of albite in the same family. In addition, the disappearance of quartz may be due to its hydrolysis by hydrothermal interactions with protons, H⁺, [22]; $\text{SiO}_2 + 2\text{H}^+ + 2\text{H}_2\text{O} \rightarrow \text{SiO}_4^{4-} + 6\text{H}^+$.

The FT-IR for same sample strongly supported the data obtained from XRD (Figure 8). The IR spectrum of the exposed sample displayed the presence of carbonation reaction-induced by-products at 1571 and 940 cm⁻¹ and the carbonate product at 1410 and 722 cm⁻¹. The amorphous carbonation product corresponds to the calcium carbonate. Assuming the following wet carbonation reactions of anorthite, $2\text{CaAl}_2\text{Si}_2\text{O}_8 + 2\text{CO}_3^- + 4\text{H}^+ \rightarrow 2\text{CaCO}_3 + \text{Al}_4\text{Si}_{4-x}\text{O}_{12-2x}(\text{OH})_4 + x\text{SiO}_2$, the carbonation by-products may be associated with the amorphous clay-like compound, Al₄Si_{4-x}O_{12-2x}(OH)₄, and amorphous

silicon dioxide. In fact, the appearance of the prominent absorption bands at 1977 and 1872 cm^{-1} was responsible for the formation of additional silicon dioxide.

Biotite

Unlike the biotite phase present in diorite mineral, the scCO_2 exposure of pure wet biotite mica mineral generated two major crystalline reaction products, sanidine [potassium aluminum silicate (KAlSi_3O_8)] in the alkali feldspar category and quartz (Figure 9). This suggested that the phase transformation of biotite into these reaction products, $\text{K}(\text{Fe},\text{Mg})_3\text{AlSi}_3\text{O}_{10}(\text{OH})_2 \rightarrow \text{KAlSi}_3\text{O}_8 + \text{SiO}_2$, is caused by its own hydrothermal reactions at 250°C [23], and is not due to scCO_2 reactions. In fact, no crystalline carbonates were found. Nevertheless, such the phase transformation entailed a conspicuous reduction of the intensity of all biotite-related d-spacing lines.

Figure 10 shows the FT-IR spectra of the exposed biotite (Figure 10). Compared with the features of the unexposed one, the spectrum of the former was characterized by the appearance of two new bands at 1980 and 1872 cm^{-1} attributed to the SiO_2 as possible quartz, and a remarkable growth of the shoulder bands at 1052, and 775 cm^{-1} to become the major ones. This growth represented an increase in the number of Si-O-Si and Al-O linkages, reflecting the formation of an alkali feldspar structure corresponding to sanidine (KAlSi_3O_8) brought about by the transformation of the mica structure. There were no bands related to amorphous carbonate products.

Therefore, among these tested minerals, the biotite was the most inert mineral to wet carbonation reactions.

Conclusions

Five rock mineral powders mixed with water, granite, albite, hornblende, diorite, and biotite, which are present in potential EGS sites, were exposed for 3 days in 250°C scCO_2 under a pressure of 17.23 MPa.

For granite, anorthoclase-type albite, one of its two existing crystalline phases was susceptible to reactions with scCO_2 . This reaction led to the formation of amorphous sodium and potassium carbonates, and clay-like minerals as the carbonation reaction-induced by-products. In contrast, the carbonation of quartz, the other phase, was minimal, if any.

The sensitivity of albite to scCO_2 reactions was much less than that of the anorthoclase-type albite, although some amorphous carbonate reaction products and by-products were formed.

The coexistence of the crystalline carbonation products, calcite and magnesite, with amorphous clay-like minerals as the reaction by-products, were noted in scCO_2 -exposed hornblende mineral, suggesting that the hornblende aggressively reacts with scCO_2 in a very short 3-day exposure period. Possibly, this reactivity is much higher than that of the anorthoclase-type albite and albite.

The diorite, which is a volcanic rock, was identified as the most valuable mineral to scCO_2 reactions. It was comprised of three crystalline phases, anorthite, biotite mica, and quartz. Upon exposure, an entire anorthite phase was eliminated from diorite, and it was converted into amorphous carbonates and clay-like reaction by-products, while the biotite mica remained intact.

Unlike the biotite phase in diorite, upon exposure, pure biotite was transformed to two crystalline phases, sanidine and quartz. No carbonation products were detected, seemingly suggesting that such phase transformation may be due to its hydrothermal reactions, but not by its carbonating reactions.

Based upon the ternary diagram of feldspars [24], the plagioclase feldspars includes albite ($\text{NaAlSi}_3\text{O}_8$), oligoclase $[(\text{Na,Ca})(\text{AlSi})\text{AlSi}_2\text{O}_8]$, andesine ($\text{NaAlSi}_3\text{O}_8$ - $\text{CaAl}_2\text{Si}_2\text{O}_8$), labradorite $[(\text{Ca,Na})\text{Al}(\text{Al,Si})\text{Si}_2\text{O}_8]$, bytownite $[(\text{NaSi,CaAl})\text{AlSi}_2\text{O}_8]$, and anorthite ($\text{CaAl}_2\text{Si}_2\text{O}_8$); these feldspars respectively contains 0-10, 10-30, 30-50, 50-70,

70-90, and 90-100 mol. % of anorthite phase. On the other hand, among the alkali feldspars are anorthoclase-type albite $[(\text{Na,K})\text{AlSi}_3\text{O}_8]$ and sanidine $(\text{KAlSi}_3\text{O}_8)$. The former alkali feldspar has 0-10 mol. % of anorthite, but the latter does not have any whatsoever. Anorthite was the most vulnerable, sensitive phase to $\text{scCO}_2/\text{water}$ reactions in the feldspar family. Thus, the carbonation rate for each feldspar mineral depends primarily on the content of anorthite. If this interpretation is valid, the magnitude of carbonation rate for feldspar minerals can be expressed in the feldspar diagram (Figure 11). As is seen, alkali feldspar minerals, which occupy as much as 60% of the earth's crust, display better performance in resisting carbonating reactions, compared with that of the plagioclase feldspar minerals. In addition, the sanidine formed by phase transformation of biotite mica is notable as the most stable phase in the $\text{scCO}_2/\text{water}$ environment at 250°C .

References

1. DOE "An Evaluation of Enhanced Geothermal Systems Technology", Geothermal Technology Program, Energy Efficiency and Renewable Energy, 2008.
2. M.O. Haring, U. Schanz, F. Ladner, and B.C. Dyer, "Characterization of the Basel 1 enhanced geothermal system", *geothermic*, 37 (2008) 469-495.
3. B. Ledesert, R.L. Hebert, C. Grall, A. Genter, C. Dezayes, D. Bartier, and A. Gerard, "Calcimertry as a useful tool for a better knowledge of flow paths in the Soutz-sous-Forets Enhanced Geothermal Systems", *J. Volcanol. Geotherm. Res.* 181 (2009) 106-114.
4. G. Zimmermann, I. Moeck, and G. Blocher, "Cyclic waterfrac stimulation to develop an Enhanced Geothermal System (EGS)-Conceptual design and experimental results", *Geothermic*, 39 (2010) 59-69.
5. T. Kohl and T. Megel, In: J. Rock Mecha. *Minn.Sci.*, "Predictive modeling of reservoir response to hydraulic stimulations at the European EGS site Soultz-sous-Forets", 44 (2007) 1118-1131.

6. S. Portier, F. Vuataz, P. Nami, B. Sanjuan, and A. Gerard, "Chemical stimulation techniques for geothermal wells: experiments on the three-well EGS system at Soultz-sous-Forets, France", *Geothermic*, 38 (2009) 349-359.
7. K. Pruess, "Enhanced geothermal systems (EGS) using CO₂ as working fluid-A novel approach for generating renewable energy with simultaneous sequestration of carbon", *Geothermic*, 35 (2006) 351-367.
8. A.H. Al-Marzouqi, A.Y. Zekri, B. Jobe, and A. Dowaidar, "Supercritical fluid extraction for the determination of optimum oil recovery conditions", *J. Petro. Sci. Eng.* 55 (2007) 37-47.
9. M. E. Parker, J.P. Meyer, and S.R. Meadows, "GHGT-9 Carbon dioxide enhanced oil recovery injection operations technologies", *Energy Procedia* 1 (2009) 3141-3148.
10. T. Sugama, N.R. Carciello, and G. Gray, "Alkali carbonation of calcium aluminate cements: Influence of set-retarding admixtures under hydrothermal conditions", *J. Mater. Sci.*, 27 (1992) 4909-4916.
11. T. Sugama and N.R. Carciello, "Carbonation of calcium phosphate cement after long-term exposure to Na₂CO₃-laden water at 250°C", *Cem. Concre. Res.*, 23 (1993) 180-190.
12. T. Sugama, "Hot alkali carbonation of sodium metaphosphate-modified fly ash/calcium aluminate blend hydrothermal cements", *Cem. Concre. Res.*, 11 (1996) 1661-1672.
13. V.C. Farmer and J.D. Russell, "The infra-red spectra of layer silicates", *Spectrochimica Acta*, 20 (1964) 1149-1173.
14. T. Uchino, T. Sakka, K. Hotta, and M. Iwasaki, "Attenuated total reflectance fourier-transform infrared spectra of a hydrated sodium silicate glass", *J. Am. Ceram. Soc.*, 72 (1989) 2173-2175.
15. T. Uchino, T. Sakka, and M. Iwasaki, "Interpretation of hydrated states of sodium silicate glasses by infrared and raman analysis", *J. Am. Ceram. Soc.*, 74 (1991) 306-313.
16. B.N. Roy, "Infrared spectroscopy of lead and alkaline-earth aluminosilicate glasses", *J. Am. Ceram. Soc.*, 73 (1990) 846-855.

17. Y. Soog, A.L. Goodman, J.R. McCarthy-Jones, and J.P. Baltrus, "Experimental and simulation studies on mineral tapping of CO₂ with brine", *Energy Conversion and Management*, 45 (2004) 1845-1859.
18. A. Berg and S.A. Banwart, "Carbon dioxide mediated dissolution of Ca-feldspar: implications for silicate weathering", *Chem. Geology*, 163 (2000) 25-42.
19. J.M. Matter and P.B. Kelemen, "Permanent storage of carbon dioxide in geological reservoirs by mineral carbonation", *Natural Geoscience*, 2 (2009) 837-841.
20. H. Lin, T. Fujii, R. Takisawa, T. Takahashi, and T. Hashida, "Experimental evaluation of interactions in supercritical CO₂/water/rock minerals system under geologic CO₂ sequestration conditions", *J. Materi. Sci.* 43 (2008) 2307-2315.
21. M.A. Trezza and A.E. Lavat, "Analysis of the system 3CaO.Al₂O₃-CaSO₄.2H₂O-CaCO₃-H₂O by FT-IR spectroscopy", *Cem. Concre. Res.*, 31 (2001) 869-872.
22. S.P. Franklin, A. Hajash Jr., T.A. Dewers, and T.T. Tieh, "The role of carboxylic acid in albite and quartz dissolution: An experimental study under diagenetic conditions", *Geochim. Cosmochim. Acta*, 58 (1994) 4259-4279.
23. M.B. Holness, "Growth and albitisation of K-feldspar in crystalline rocks in the shallow crust: a new kind of porosity?", *J. Geochem. Explor.*, 78 (2003) 173-177.
24. J.R. Prescott and P.J. Fox, "Three-dimensional thermoluminescence spectra of feldspars", *J. Phys.D: Appl. Phys.* 26 (1993) 2245-2254.

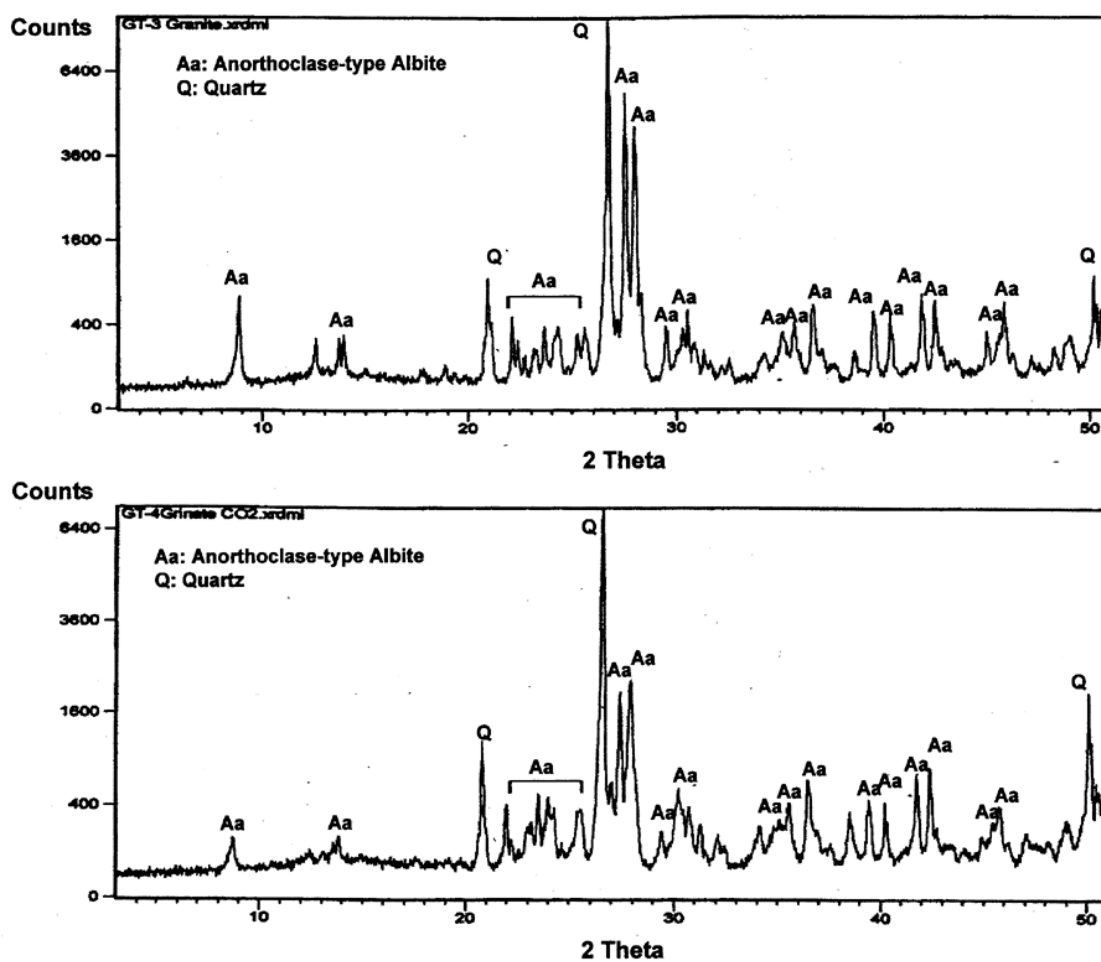


Figure 1. XRD patterns for granite mineral before (top) and after (bottom) exposure to $scCO_2$ /water.

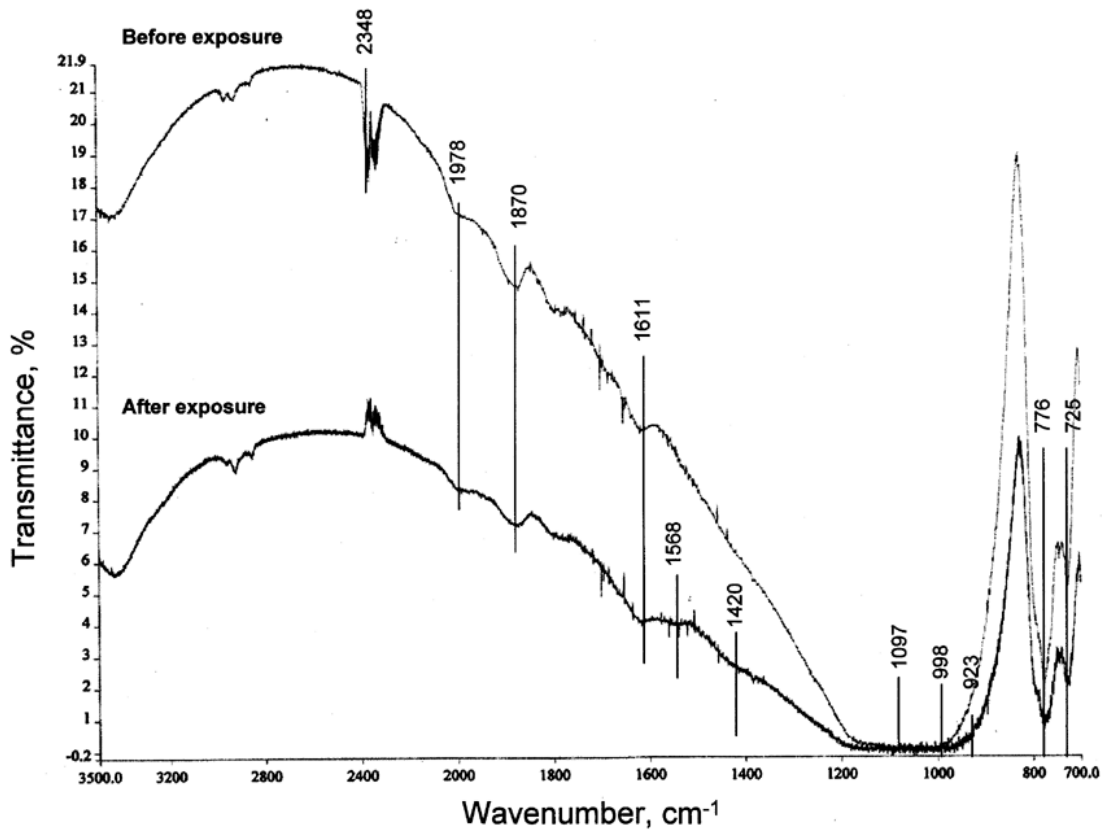


Figure 2. FT-IR spectra for unexposed and exposed granite to scCO₂/water.

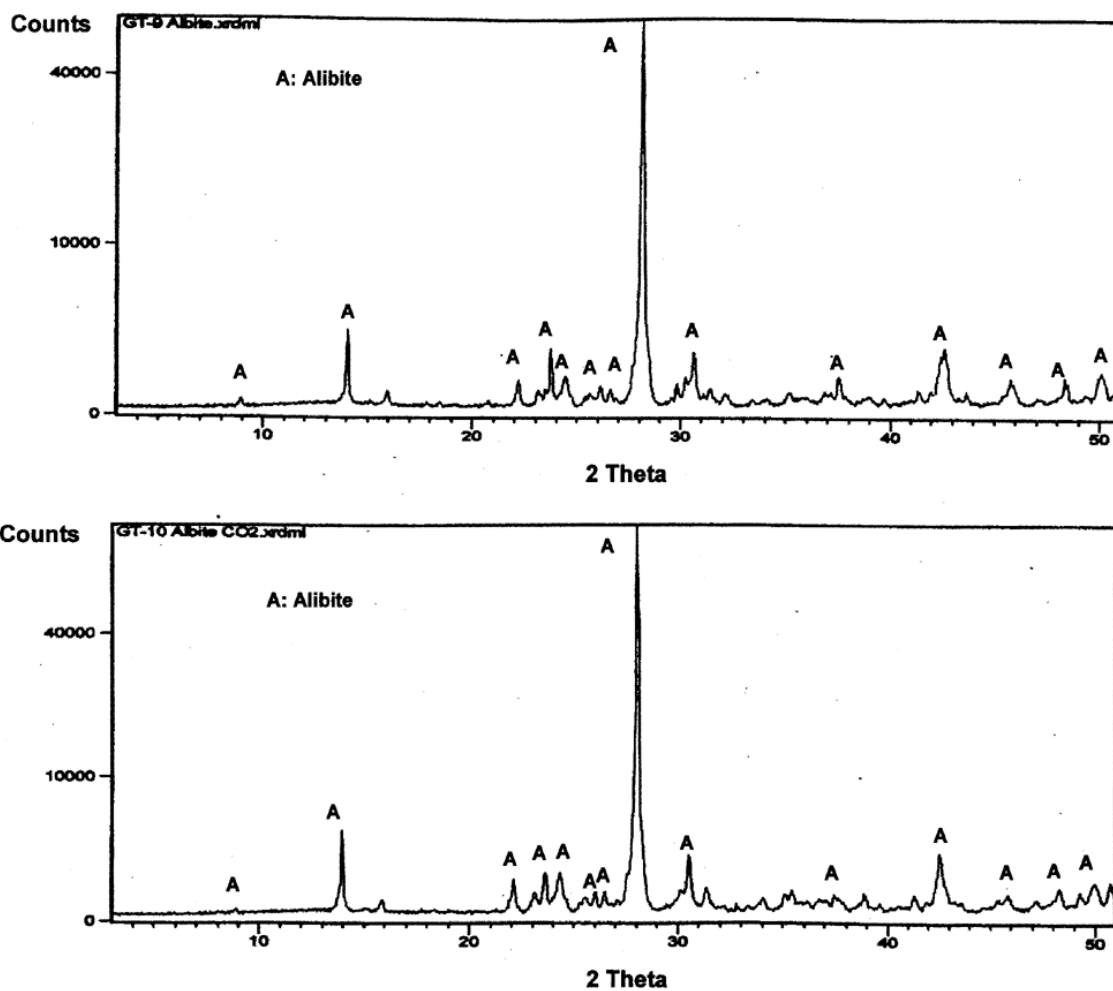


Figure 3. XRD tracings for alibite before (top) and after (bottom) exposure to scCO₂/water.

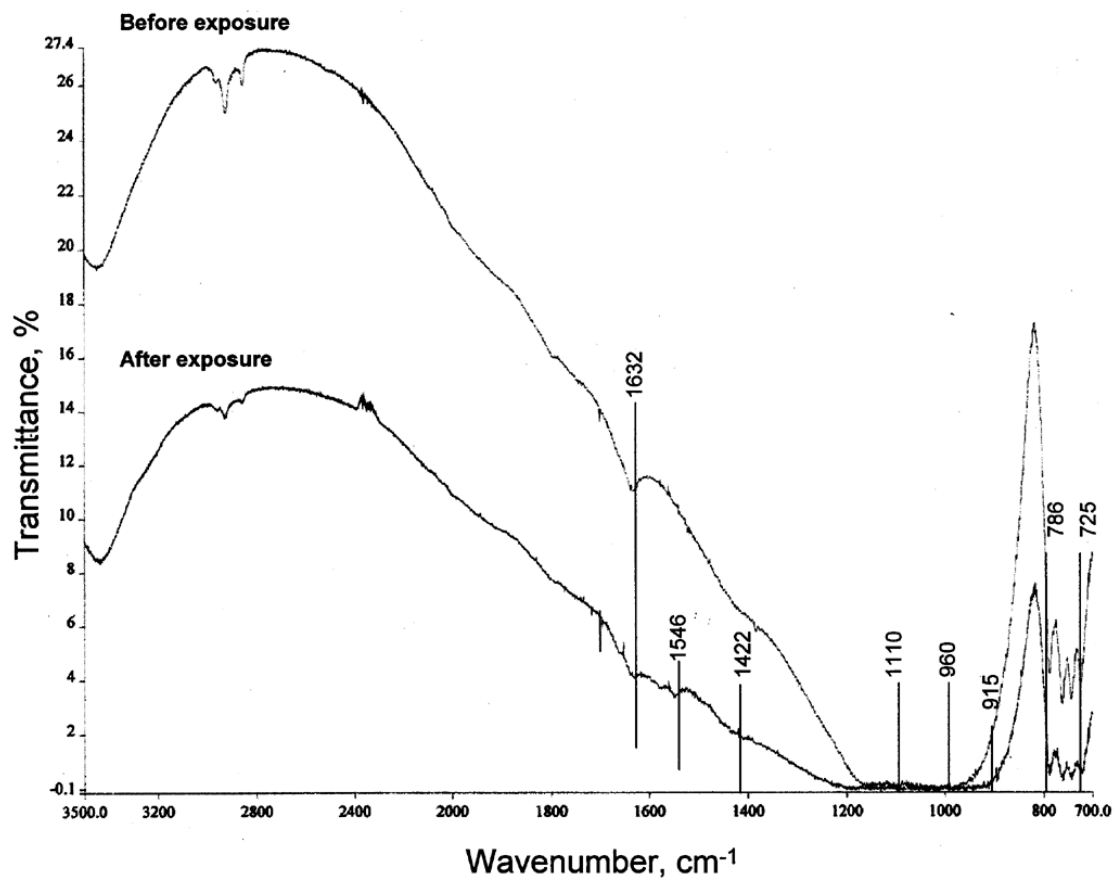


Figure 4. FT-IR spectra for unexposed and exposed albite.

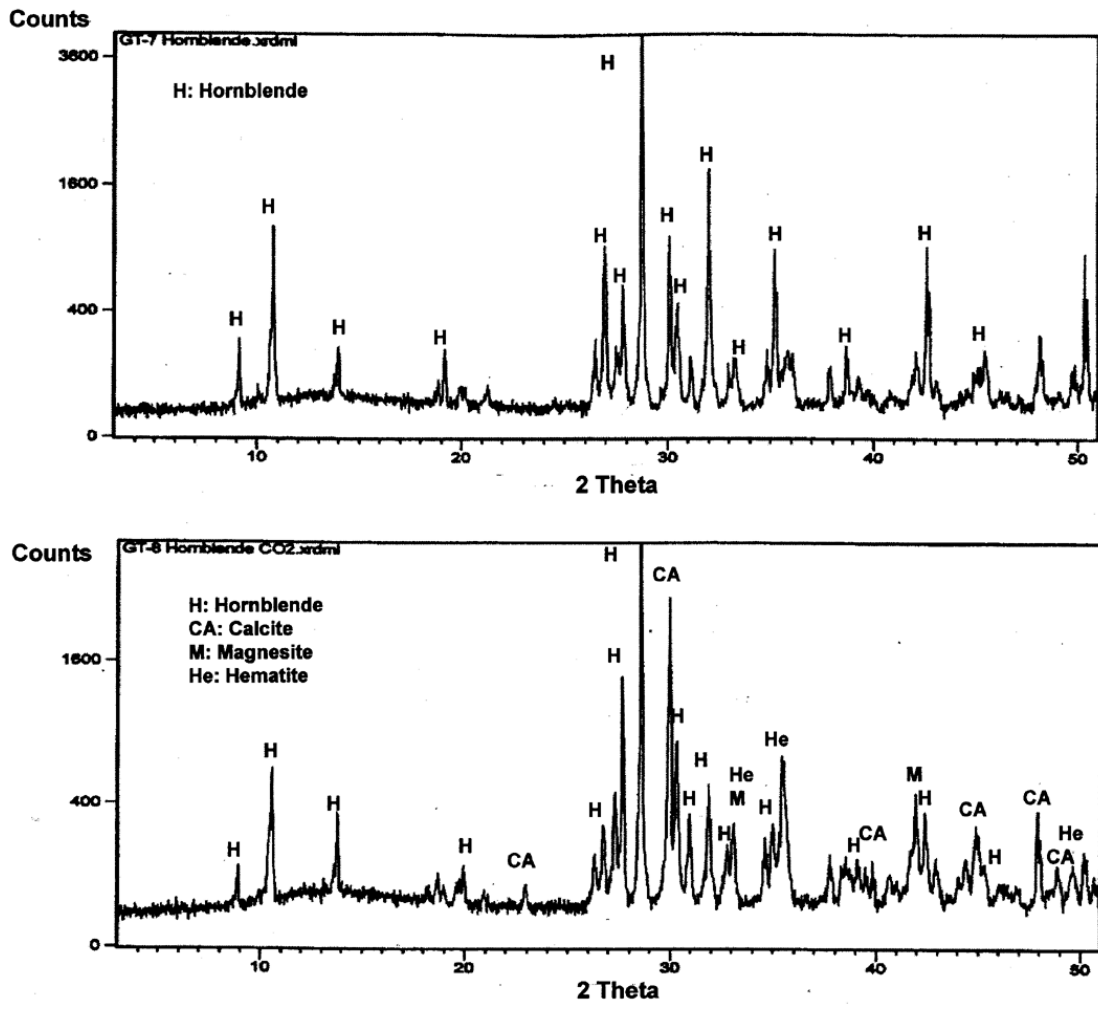


Figure 5. XRD results for hornblende before (top) and after (bottom) exposure.

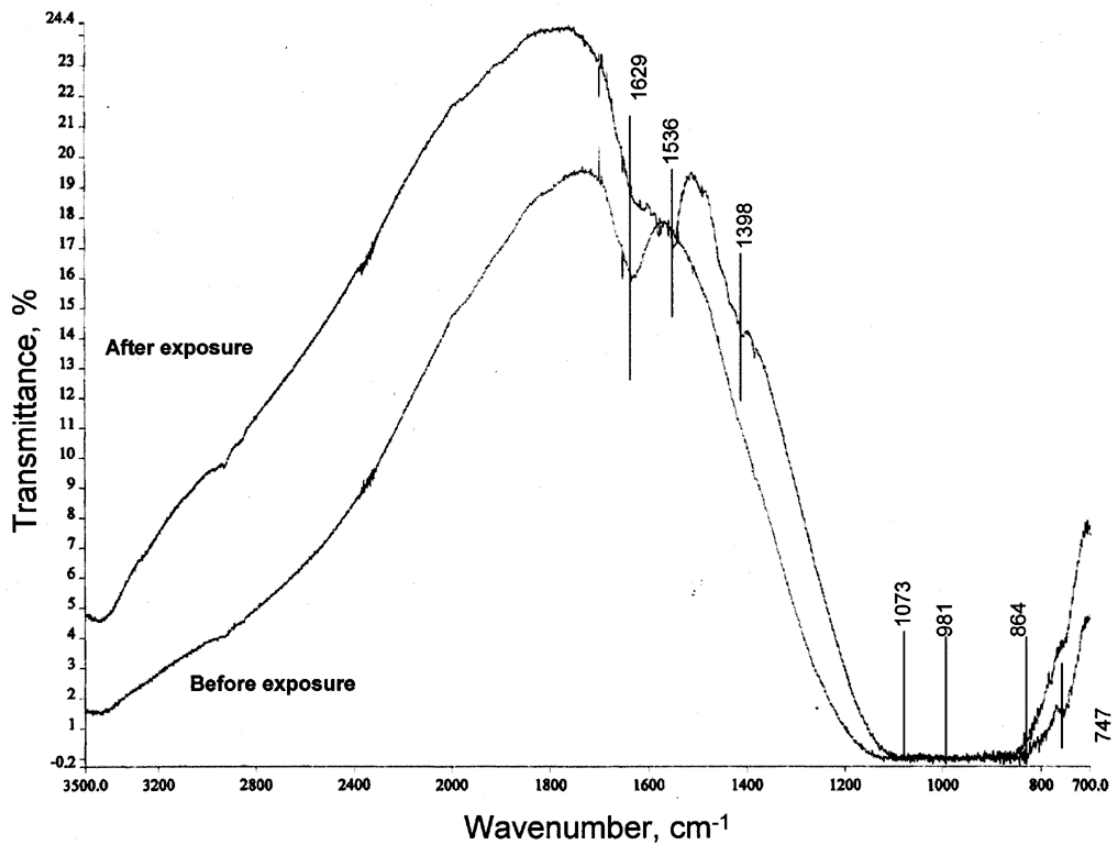


Figure 6. FT-IR spectra for unexposed and exposed hornblende.

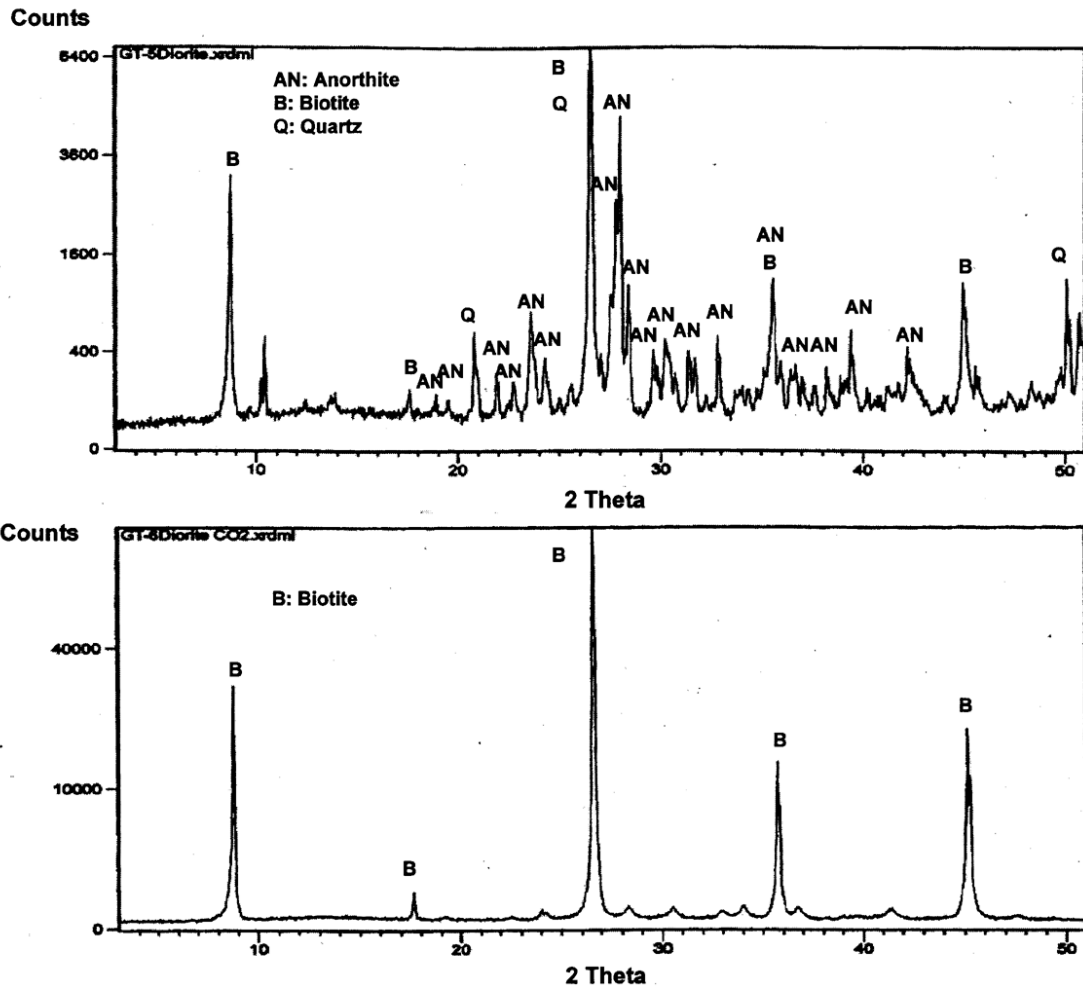


Figure 7. XRD data for diorite before (top) and after (bottom) exposure.

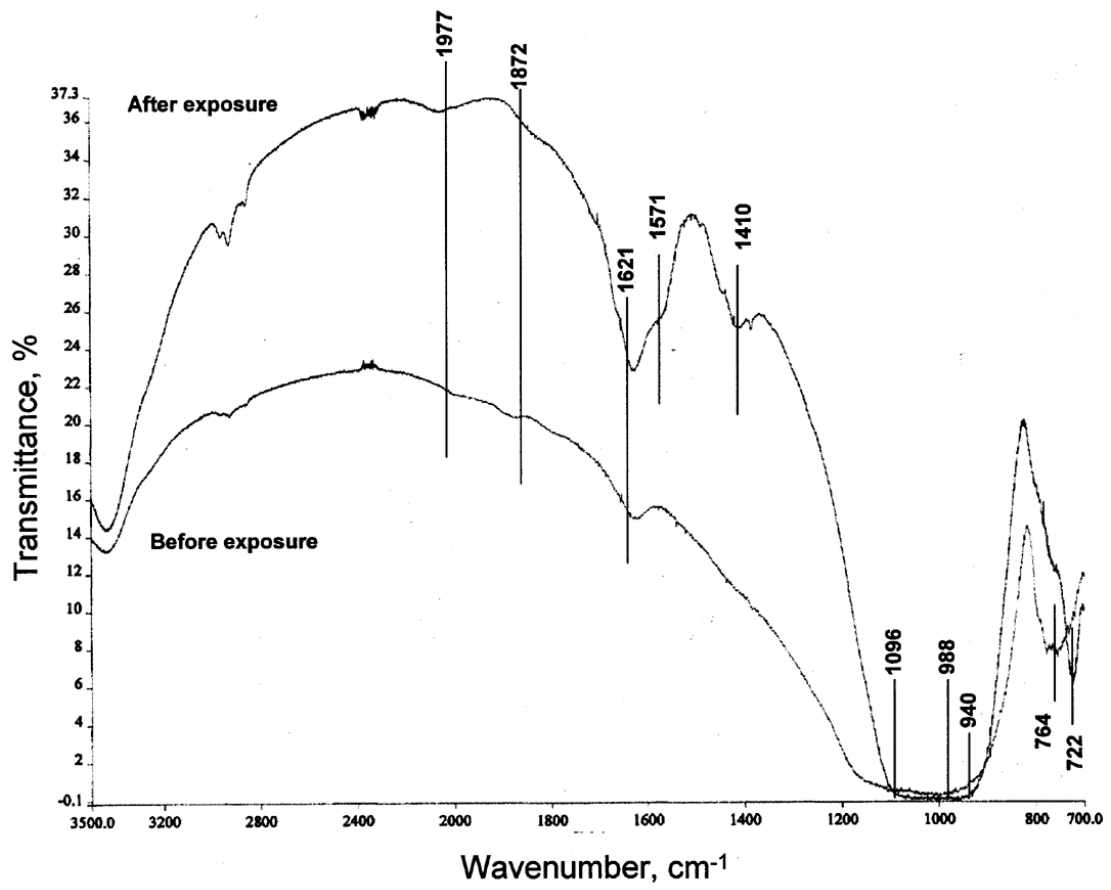


Figure 8. FT-IR results from unexposed and exposed diorite.

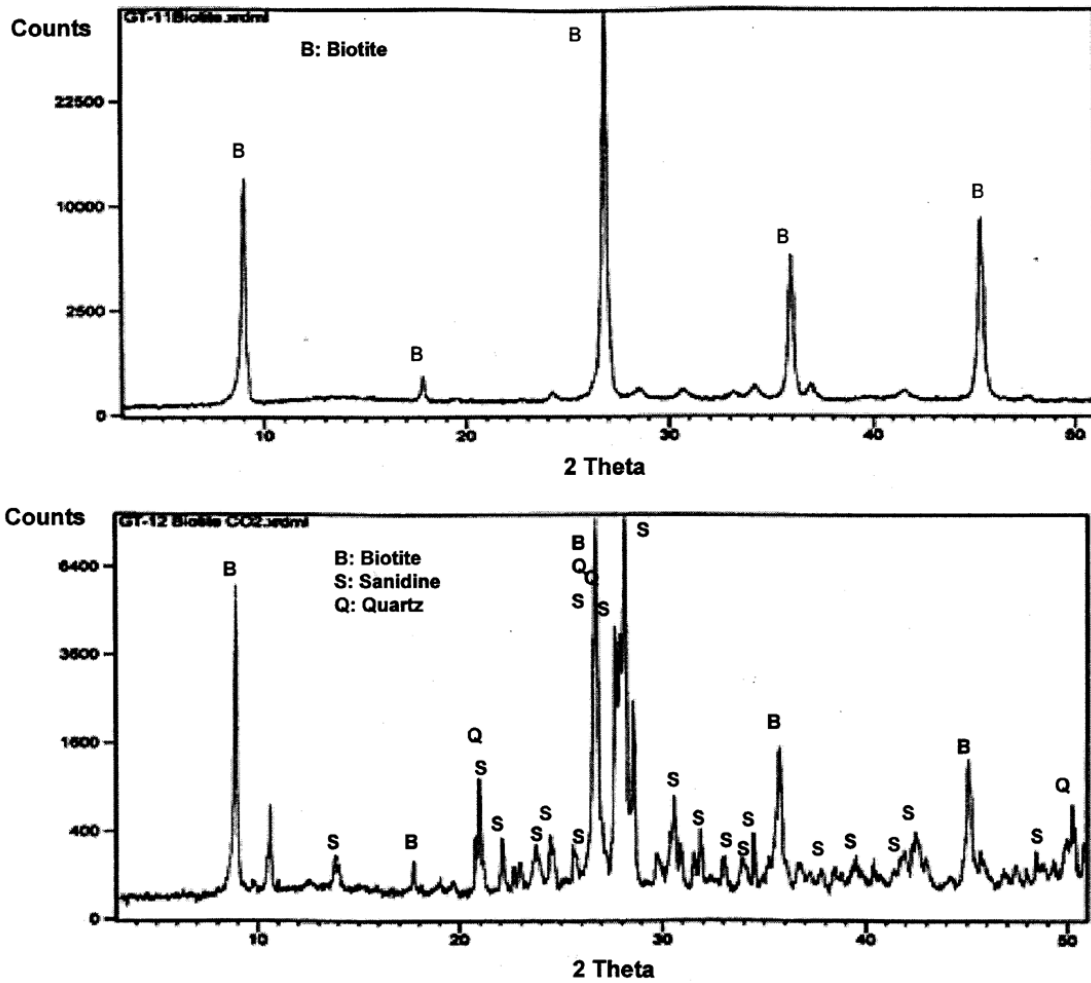


Figure 9. XRD patterns for biotite before (top) and after (bottom) exposure.

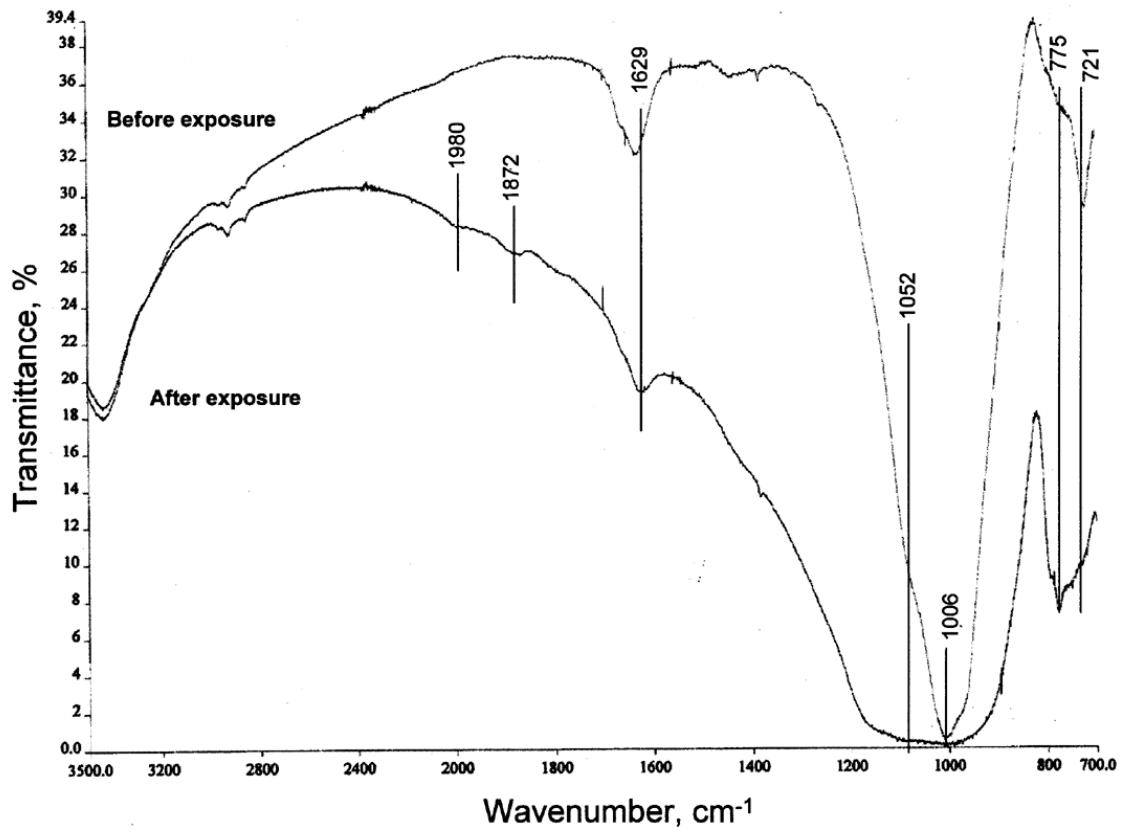


Figure 10. Comparison of FT-IR spectral features between unexposed and exposed biotite.

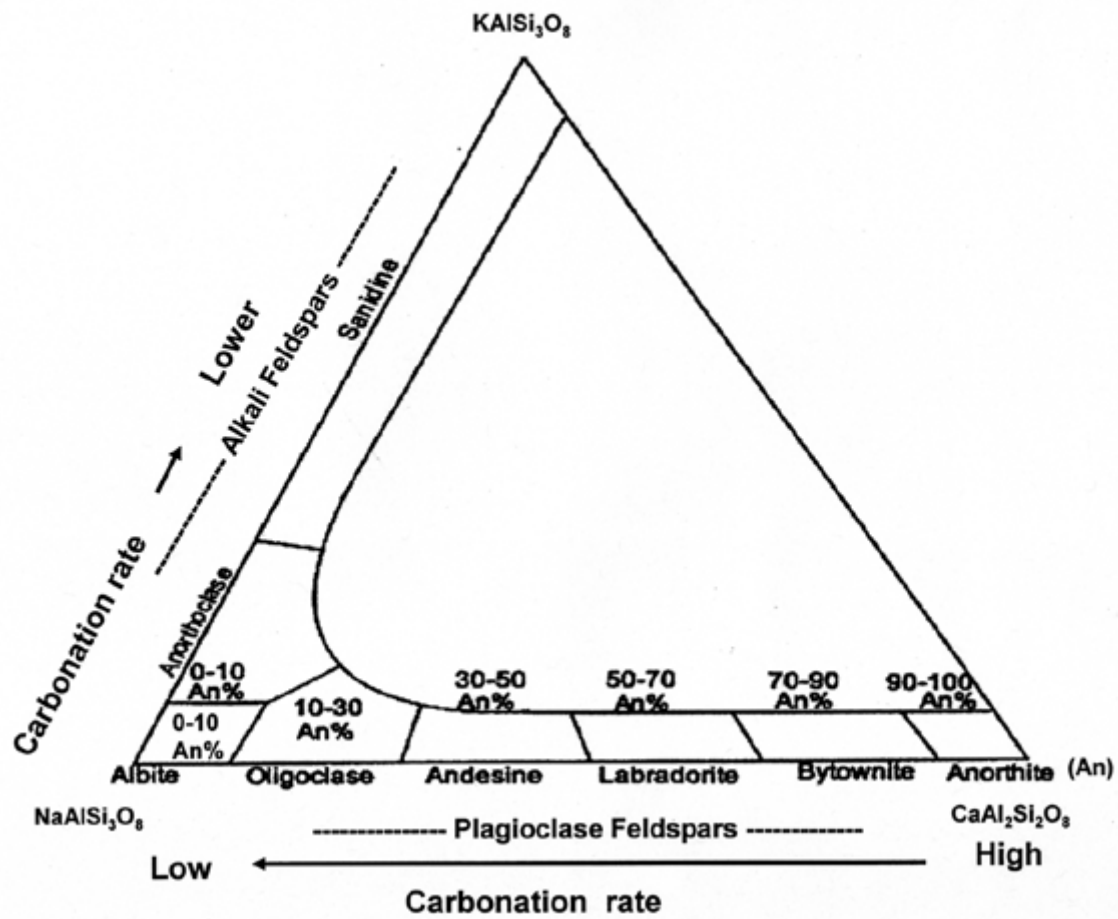


Figure 11. Tendency of various different feldspar minerals to carbonation based upon the feldspar ternary diagram.